Poly(styrene-*b*-methyl methacrylate) block copolymers as compatibilizing agents in blends of poly(styrene-*co*-acrylonitrile) and poly(2,6-dimethyl-1,4-phenylene ether): 2. Influence of concentration and molecular weight of symmetric block copolymers

Clemens Auschra and Reimund Stadler*
Institut für Organische Chemie, Johannes-Gutenberg-Universität, J. Becherweg 18–20, W-6500 Mainz, Germany

and Ingrid G. Voigt-Martin
Institut für Physikalische Chemie, Johannes-Gutenberg-Universität, Welderweg, W-6500 Mainz, Germany
(Received 24 August 1992)

The influence of the molecular weight of the symmetric block copolymer poly(styrene-*b*-methyl methacrylate) (P(S-*b*-MMA)) in blends with high-molecular-weight poly(styrene-*co*-acrylonitrile) (PSAN) and poly(2,6-dimethyl-1,4-phenylene ether) (PPE) is investigated by dynamic mechanical analysis and transmission electron microscopy. Total molecular weights of the block copolymers vary from 16 up to 275 kg mol^{-1}. Independent of molecular weight, all block copolymers locate to the interface with strong dispersing efficiency. The different block copolymers also showed approximately the same emulsifying efficiency. The degree of segmental mixing of the blocks with the respective phases is evaluated from the glass transition behaviour. A qualitative model is developed to relate the observed glass transition behaviour to the segmental distribution. In blends with large block copolymers, polystyrene blocks and PPE are rather uniformly mixed. The degree of mechanical coupling of the phases increases with the block copolymer molecular weight. The favourable enthalpic interaction between the blocks and the blend components is a major factor determining the phase behaviour. In contrast to this, the molecular weight of PPE showed little influence on blend behaviour.

(Keywords: block copolymers; compatibilizers; blends; poly(styrene-*b*-methyl methacrylate); poly(styrene-*co*-acrylonitrile); poly(phenylene ether); symmetric blocks; concentration dependence; molecular-weight dependence)

INTRODUCTION

The mechanical performance of multiphase polymer alloys strongly depends on morphology and phase adhesion[1,2]. It is often difficult to control these features owing to the marked incompatibility of many blend components[3]. The use of appropriate interfacial agents like block or graft copolymers is good practice to improve blend properties[4]. Compatibilizers with high efficiency are essential for tailoring of blend properties. Both theory[5–9] and experiment[10–15] have demonstrated the importance of structural variables, i.e. block architecture, chemical composition and molecular weight, for compatibilizing efficiency.

In the first paper of this series[16] we investigated the location of a symmetric high-molecular-weight poly(styrene-*b*-methyl methacrylate) (P(S-*b*-MMA) or SM) diblock copolymer in blends of poly(styrene-*co*-acrylonitrile) (PSAN) and poly(2,6-dimethyl-1,4-phenylene ether) (PPE). Dynamic mechanical analysis and TEM observation demonstrated that in blends with PSAN20 (=20 wt% acrylonitrile) the block copolymers locate only to the interface. No formation of micelles could be detected up to high concentrations of block copolymers. Besides a possible technical relevance of this system, it represents a model system A/C-D/B, in which the blocks of the compatibilizer are chemically different from, but thermodynamically miscible with, one of the blend components. This additional thermodynamic driving force for mixing of the blocks with the respective blend components leads in some respects to a different behaviour, if compared with systems A/A-B/B, where the block copolymer has the same constituents as the blend components. A stronger tendency for location to the interface and lower tendency to form micelles is observed[15]. Such behaviour is advantageous for a systematic investigation on molecular-weight effects of block copolymers attached to interfaces. Recently, much attention has focused on systems with tethered chains extending into homopolymer phases with special

* To whom correspondence should be addressed

0032-3861/93/102094-17

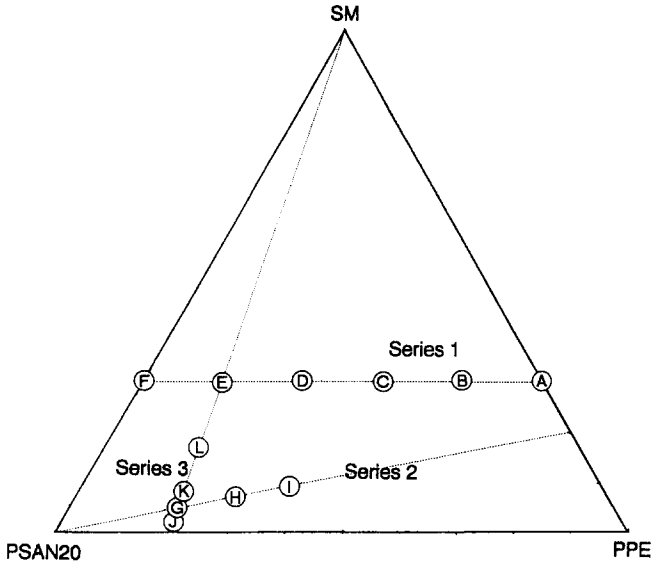

Figure 1 Composition diagram showing the different blend series of ternary blends PSAN20/PPE/P(S-*b*-MMA)

emphasis on the segmental distributions[8,14,17–19]. In the case of an A/C-D/B blend system the extent of segmental mixing of the block copolymer chains with the phases A and B changes their glass transition behaviour and can be investigated by dynamic mechanical spectroscopy.

In this contribution we report on the influence of the molecular weight of symmetric P(S-*b*-MMA) block copolymers at different concentrations in ternary blends with high-molecular-weight PSAN20 and PPE. The block lengths of the copolymers vary in the range from 8000 to 120 000 g mol^{-1}. Dynamic mechanical analysis is used to characterize the composition of the phases, the interphase and the degree of mechanical coupling. Morphology is examined by transmission electron microscopy. In the first part we give the dynamic mechanical analysis of ternary blends with PSAN20 matrix and a dispersed PS/PPE phase, as well as blends with PSAN20/PMMA matrix and a dispersed PPE phase. The behaviour of these model blends with a uniformly mixed PS/PPE phase and a uniformly mixed PSAN20/PMMA phase will serve as reference to interpret the dynamic mechanical behaviour of ternary blends PSAN20/PPE/P(S-*b*-MMA) in terms of the degree of segmental mixing of the block copolymers with the component phases.

Three blend series outlined in *Figure 1* and defined in *Table 4* will be discussed. In series 1, the ratio of PSAN20 to PPE is varied in blends with a high-molecular-weight block copolymer at fixed block copolymer concentration of 30 wt%. In series 2, the ratio of different P(S-*b*-MMA) block copolymers to PPE is kept constant while changing the amount of the main component PSAN20. In the last series 3, the total amount of block copolymer is strongly increased at constant ratio PSAN20/PPE of 80:20. For this series, a quantitative morphological analysis will be given for some representative blends to characterize the dispersing efficiency of different block copolymers. The observed dynamic mechanical and morphological behaviour will be discussed in terms of a qualitative model describing the extent of segmental mixing between the component phases and the block copolymers. In the last section, blends with a lower-molecular-weight PPE are investigated, in order to evaluate the influence of the PPE molecular weight on the segmental distribution of PS block chains and PPE.

EXPERIMENTAL

Materials

P(S-b-MMA). These block copolymers were prepared by sequential anionic polymerization as described elsewhere[16]. All block copolymers have narrow molecular-weight distributions. The amount of terminated homopolystyrene is always negligible. Detailed g.p.c. analysis demonstrates that in these block copolymers a few per cent by weight of homopolystyrene can be detected, if present[20].

PSAN20 and PPE. These were grossly fractionated high-molecular-weight samples, the same materials as in our previous paper[16].

Analytical results of molecular weight and composition are summarized in *Tables 1* and *2*. In comparison with the other block copolymers, SM120 is slightly asymmetric. The low-molecular-weight block copolymer SM8 is not microphase-separated in bulk.

Blend preparation and testing

All blends were prepared by coprecipitation from dilute

Table 1 Characterization of block copolymers[a]

	PS block[b]		P(S-*b*-MMA)		
Copolymer SM*xx*	M_n (kg mol^{-1})	M_w/M_n	M_n[c] (kg mol^{-1})	M_w/M_n	w_{PS}[d]
SM8	8	1.05	(16)	1.09	0.44
SM25	25	1.09	(52)	1.18	0.46
SM43	43	1.09	(73)	1.12	0.48
	48[e]		105[e]		
SM78	78	1.09	(136)	1.09	0.47
	78[e]		155[e]		
SM97	97	1.12	(180)	1.13	0.47
	92[e]		205[e]		
SM120	120	1.11	(233)	1.11	0.40
	128[e]		275[e]		

[a] Molecular weights from g.p.c. (PS calibration)
[b] A small sample of the PS block was taken from the reactor after polymerization of styrene
[c] G.p.c. molecular weights of the block copolymers in parentheses are somewhat too low due to PS calibration
[d] Weight fraction PS from ^{1}H n.m.r.
[e] Molecular weights from membrane osmometry with toluene or $CHCl_3$ as solvent

Table 2 Characterization of blend components

Polymer	M_n (kg mol^{-1})	M_w/M_n	w_{PS}[d]
PSAN20	(166)[a]	1.60[a]	0.89[d]
	160[c]		
PPE-II	(105)[b]	2.0[b]	0
	90[c]		
PPE-III	25[b]	2.0[b]	0
PS[e]	100[a]	1.04[a]	1
PMMA[e]	220[a]	1.16[a]	0

[a] G.p.c., tetrahydrofuran (THF) PS calibration
[b] G.p.c., $CHCl_3$ PS calibration
[c] Membrane osmometry, $CHCl_3$
[d] Weight fraction PS from elemental analysis
[e] Anionically synthesized in THF

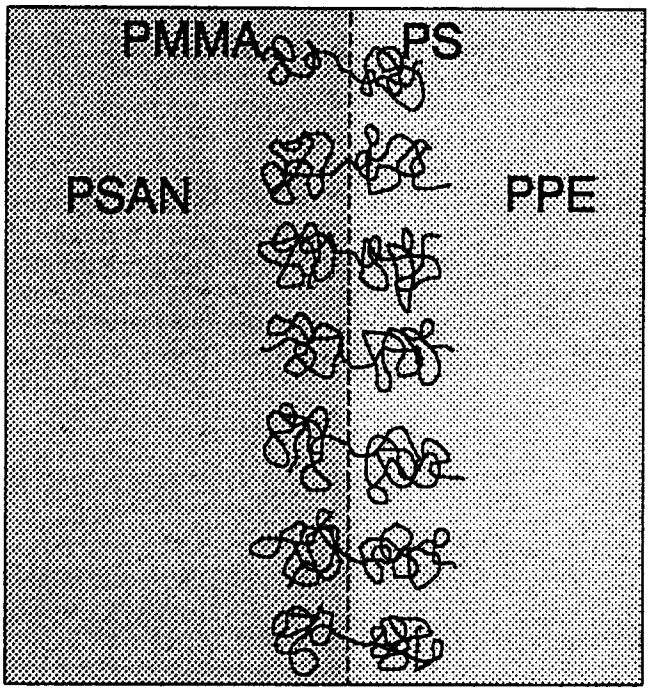

Figure 2 Schematic representation of the interfacial situation in ternary blends of PSAN20/PPE/P(S-*b*-MMA)

solution and subsequent melt pressing at 240°C for 45 min. These conditions ensure approach to equilibrium without degradation of PMMA. For details see ref. 16.

Dynamic mechanical testing

This was performed with a Rheometrics Solids Analyzer RSAII in the temperature-step mode at a constant frequency of 1 rad s^{-1} with the dual cantilever and the shear sandwich test fixtures, to cover a broad range of moduli, exactly in the same way as described in our previous paper[16].

TEM analysis

Ultrathin sections of samples were microtomed with a diamond knife at room temperature and stained with RuO_4 vapour as described earlier[16].

RESULTS AND DISCUSSION

Interfacial situation

The extent of segmental mixing of the blocks of the copolymers with the respective phases will be reflected in the glass transition behaviour. According to *Figure 2* the block copolymers will be located at the interface. The PMMA blocks extend into the PSAN20 phase, while the PS blocks extend into PPE phase. The uniformity of the segmental mixing is restricted by the confinement of the junction points to the interfacial region. This situation corresponds to two layers of PS and PMMA chains tethered to the same surface and extending in opposing directions into different phases. The interaction of these brushes with the phases, i.e. the extent of segmental mixing, can be expected to depend on block copolymer molecular weight and will be analysed by d.m.a.

D.m.a. of model blends with one phase consisting of two homogeneously mixed components

As a reference state ensuring unrestricted mixing of PMMA chains with PSAN20 and PS chains with PPE, two model blend series (*Table 3*) were investigated. *Figure 3* shows the dynamic mechanical behaviour of ternary blends PSAN20/(PS/PPE) (80:20). The matrix PSAN20 is immiscible with both PS and PPE, whereas PS and PPE are miscible at all compositions and therefore form a homogeneously mixed phase. The glass transition of this dispersed PS/PPE phase according to the maximum of tan δ, shows the same composition dependence as simple binary PS/PPE blends and can be described by the Gordon–Taylor equation[21] (broken curve in *Figure 8*; PPE, $\tan\delta_{max}=227°C$; PS, $\tan\delta_{max}=110°C$; Gordon–Taylor constant $K=0.79$):

$$T_g=\frac{w_{PS}T_g(PS)+Kw_{PPE}T_g(PPE)}{w_{PS}+Kw_{PPE}} \quad (1)$$

with w_{PS} and w_{PPE} the weight fractions of PS and PPE.

Besides the reduction in temperature of $\tan\delta_{max}$, the blends with mixed PS/PPE phase (curves 2–5 in *Figure 3*) show some broadening of the glass transition in comparison with the binary blend PSAN20/PPE (80:20) with pure PPE (upper curve 1 in *Figure 3*).

If the temperature of the maximum of the G'' peak is taken as a measure of T_g, the composition dependence is also adequately described by equation (2). In blends with significantly broadened glass transitions of the dispersed mixed PS/PPE phase, as in blends with some block copolymers, the maximum (or centre) of the G'' peak is more difficult to assign than the maximum of tan δ. Therefore, in the following discussion, the T_g analysis of the mixed PS/PPE phase will be mainly based upon the variation of tan δ.

Figure 4 shows the dynamic mechanical analysis of blends (PSAN20/PMMA)/PPE (70/30) with a homogeneously mixed matrix of PSAN20 and PMMA and a dispersed PPE phase. In these compositions the whole range of the glass transition of the mixed PSAN20/PMMA phase is accessible with the dual cantilever test fixture. With increasing amounts of PMMA, the glass transition shifts to higher temperatures and is broadened. The temperature shift of T_g with composition of the PSAN20/PMMA phase is smaller compared with the PS/PPE phase because the difference in T_g is smaller. Taking the maximum of E'' as a measure of T_g, the variation of T_g with composition can also be properly described by the Gordon–Taylor equation (broken curve in *Figure 6*; PSAN20, $E''_{max}=107°C$; PMMA,

Table 3 Compositions of model blends. Model blends with one phase consisting of two components homogeneously mixed (weight ratios)

Blend No.	PSAN20	PS	PPE-II	w_{PS}[a]
1	80	0	20	0
2	80	2	18	0.1
3	80	4	16	0.2
4	80	6	14	0.3
5	80	8	12	0.4
Blend No.	**PSAN20**	**PMMA**	**PPE-II**	w_{PMMA}[b]
6	70	0	30	0
7	56	14	30	0.2
8	42	28	30	0.4
9	28	42	30	0.6
10	14	56	30	0.8
11	0	70	30	1

[a] w_{PS} = weight fraction of PS on the basis of PS/PPE
[b] w_{PMMA} = weight fraction PMMA on the basis of PSAN20/PMMA

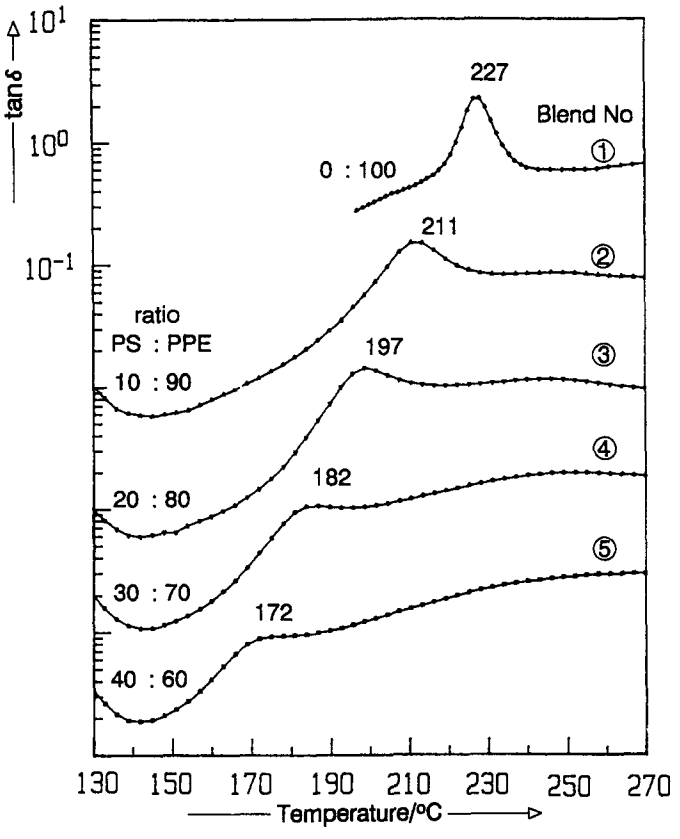

Figure 3 Analysis of the glass transition of the homogeneously mixed PS/PPE phase in model blends PSAN20/(PS/PPE(x/y))(80/20) according to tan δ; measurements were made with the shear sandwich test fixture

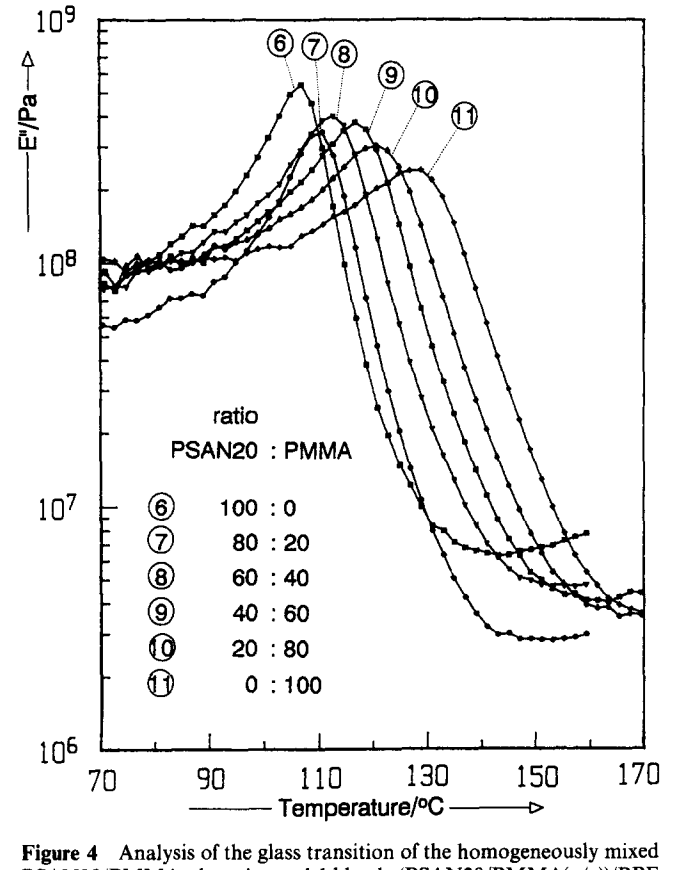

Figure 4 Analysis of the glass transition of the homogeneously mixed PSAN20/PMMA phase in model blends (PSAN20/PMMA(x/y))/PPE (70/30) according to E''; measurements were made with the dual cantilever test fixture; values for T_g and half-height widths are given in *Table 5*

$E''_{max} = 129°C$; $K = 0.60$). The Gordon–Taylor equation also works well, if the temperature of tan δ_{max} is chosen as a measure for T_g. Parallel to the increase in T_g, the E'' and tan δ peaks get broadened. As can be seen from *Table 5* and *Figure 7*, the half-height widths continuously increase as the PMMA content is raised.

Dynamic mechanical analysis of blend series 1

Blend series 1 consists of ternary blends with the high-molecular-weight block copolymer SM97. The ratio of PSAN20 to PPE is varied, while the amount of SM97 is kept relatively high at a constant value of 30 wt%. Thus, going from composition A to composition F (see *Figure 1* and *Table 4*) both the ratio of PPE to PS, as well as the ratio PSAN20/PMMA, vary over a broad range. Therefore, the influence of added block copolymer on the glass transitions should be detectable in this series, if significant mixing of block chains and the corresponding blend components occurs.

Figure 5a and *5b* show the dynamic mechanical behaviour of these blends. According to E'' and tan δ, the PSAN20 glass transition is shifted to higher temperatures as the ratio of PMMA to PSAN20 is increased (see also *Table 5*). This T_g shift is comparable with the T_g shift observed in the model blends with homogeneously mixed PSAN20/PMMA phase and proves the mixing of PMMA blocks with PSAN20. In *Figure 6* the T_g values $T_g(E''_{max})$ of these blends are plotted against the composition PSAN20/PMMA and compared with the T_g values of the blends with homogeneously mixed PSAN20/PMMA phase. Both sets of data are well described by the same T_g–composition relation. The analysis of the width of the PSAN20 glass transition gives information about the uniformity of segmental mixing.

Figure 7a (see also *Table 5*) shows the tan δ half-height widths of the PSAN20 glass transition for the blends of series 1 as a function of the PSAN20/PMMA composition, in comparison with the model blends. The tan δ half-height widths roughly follow the same trend in both series with a small positive deviation in the intermediate composition range. Looking at the E'' half-height widths (*Figure 7b*), this deviation is very pronounced for the blends C and D. This is indicative of a rather non-uniform segmental distribution of PSAN20 and PMMA blocks in these blends. Thus, the

Table 4 Compositions of ternary blends with P(S-*b*-MMA)

Composition	PSAN20	PPE-II	P(S-*b*-MMA)	w_{PMMA}[a]	w_{PS}[b]
Series 1 (SM97)					
A	0	70	30	1	0.17
B	14	56	30	0.53	0.20
C	28	42	30	0.36	0.25
D	42	28	30	0.27	0.33
E	56	14	30	0.22	0.50
F	70	0	30	0.19	1
Series 2 (xx = 8–120)					
G_{SMxx}	80	20	5	≈0.03	≈0.11
H_{SMxx}	70	30	7.5	≈0.05	≈0.11
I_{SMxx}	60	40	10	≈0.08	≈0.11
Series 3 (xx = 8–120)					
J_{SMxx}	80	20	2.5	≈0.02	≈0.06
G_{SMxx}	80	20	5	≈0.03	≈0.11
K_{SMxx}	80	20	10	≈0.06	≈0.20
L_{SMxx}	80	20	20	≈0.11	≈0.33

[a] w_{PMMA} = weight fraction of *b*-PMMA on the basis of *b*-PMMA/PSAN20
[b] w_{PS} = weight fraction of *b*-PS on the basis of *b*-PS/PPE

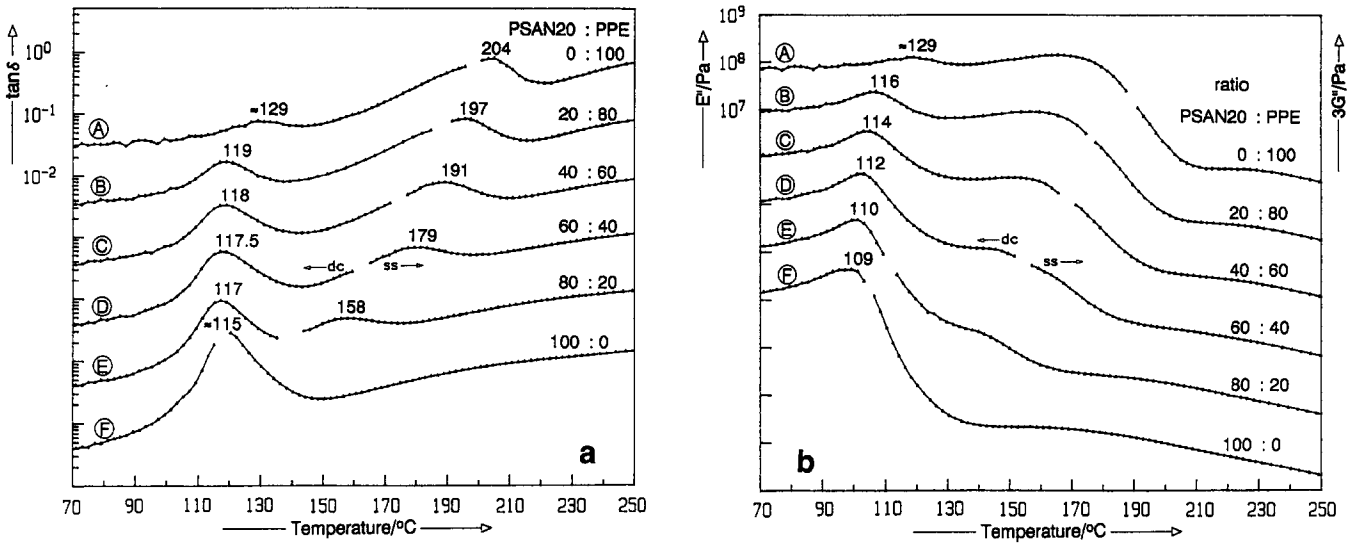

Figure 5 (a) The tan δ analysis of blend series 1 consisting of ternary blends (PSAN20/PPE(x/y))/SM97 (70/30). Data on the left-hand side correspond to measurements with the dual cantilever test fixture (dc), data on the right correspond to the shear sandwich test fixture (ss). (b) The E'' analysis of blend series 1. For better comparison, the shear modulus data (ss) are converted to E'' data according to the relation[16] $E''=3G''$. Curves for the different blends are vertically offset against each other by one decade

Table 5 Analysis of the glass transition of the mixed PSAN20/PMMA phase in different blends

No.	w_{PMMA}[a]	E'' peak		tan δ peak	
		T (°C)[b]	Width (°C)[c]	T (°C)[d]	Width (°C)[e]
Model blends (PSAN20/PMMA(x/y))/PPE (70/30)					
6	0	107	10.2	111	10.0
7	0.2	110	10.7	115	13.5
8	0.4	113	13.5	119	14.5
9	0.6	118	14.2	124	15.2
10	0.8	122	16.6	129	17.7
11	1	129	17.9	136	18.3
Blend series 1					
F	0.19	109	–[f]	114	–[f]
E	0.22	110	11.9	117	12.6
D	0.27	112	17.7	117.5	14.6
C	0.36	114	18.5	118	15.3
B	0.53	116	15.0	119	15.0
A	1	129	–[g]	≈129	–[g]

[a] Weight fraction PMMA corresponding to the ratio of PSAN20 to PMMA in the blend
[b] Temperature of the maximum of the E'' peak
[c] Half-height width of the E'' peak; a line parallel to the temperature abscissa through the E'' curve at 70°C was used as arbitrary baseline to define the E'' peak
[d] Temperature of the maximum of the tan δ peak
[e] Half-height width of the tan δ peak, drawing the baseline as tangent, connecting the beginning and the end of the peak
[f] In this blend the whole PSAN20 glass transition peak was not accessible with the dual cantilever test fixture
[g] PMMA glass transition too weak to determine realistic values for the half-height widths

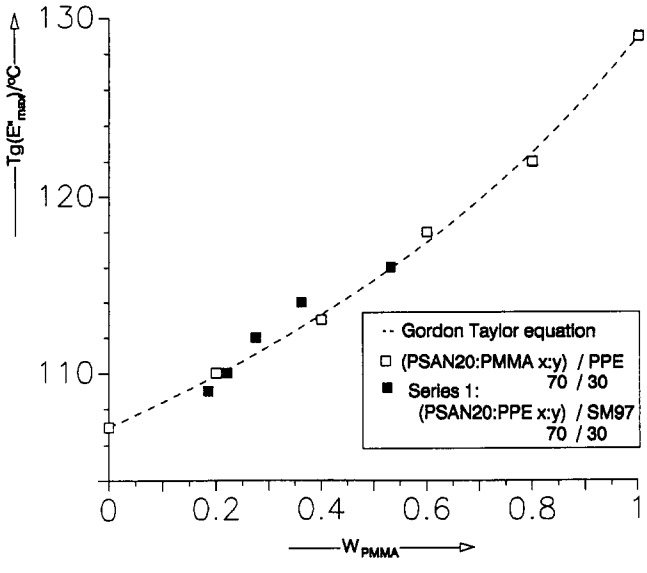

Figure 6 $T_g(E''_{max})$ of the mixed PSAN20/PMMA phase in different blends plotted against the composition of PSAN20/PMMA. The broken curve gives the predictions of the Gordon–Taylor equation ($K=0.6$, T_g(PSAN20) = 107°C, T_g(PMMA) = 129°C)

behaviour of the PSAN20 glass transition in blends of series 1 is consistent with the picture that the PMMA blocks of the block copolymer SM97, which is located at the interface, and PSAN20 are extensively mixed. In some compositions, the broadening of the glass transition indicates significant variations in segmental distribution across the PSAN20 phase. The same analysis can be made for the PPE glass transition. *Figures 5a* and *5b* show that the PPE glass transition is significantly lowered as the ratio of PPE to PS drops, i.e. in going from composition A to composition E. The temperature reduction in T_g is comparable to blends with homogeneously mixed PS/PPE phase.

Figure 8 compares the $T_g(\tan\delta_{max})$ of the PS/PPE mixed phase of the blends in series 1 with the model blends having homogeneously mixed PS/PPE phase (also included are the T_g values of blends of series 3 with SM97 and SM120). For these blends, the variation of T_g with composition for the mixed PS/PPE phase is well described by the Gordon–Taylor equation. Also the widths of the tan δ peaks are comparable to the model blends with homogeneously mixed PS/PPE phase (compare *Figure 5a* with *Figure 3*). Here we give no quantitative analysis in terms of half-height widths, because the whole transition could not be covered by a single testing geometry (i.e. the shear sandwich test fixture) and we have no reliable procedure to set the baseline to define the E'' peak. Nevertheless, it is clear

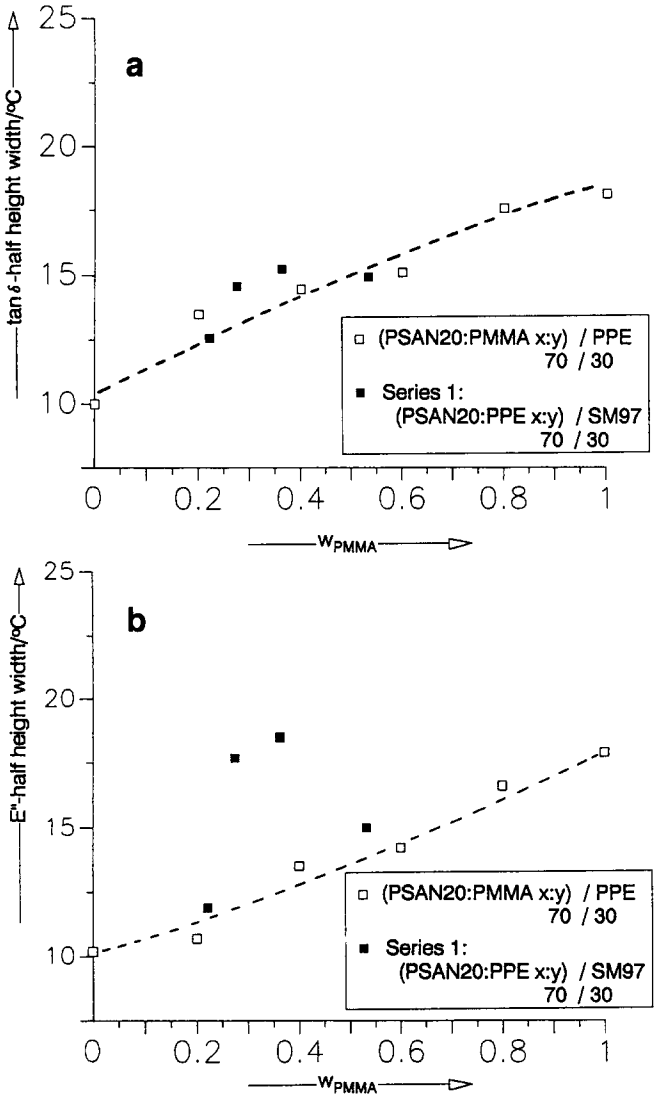

Figure 7 Analysis of (a) the tan δ half-height widths and (b) the E'' half-height widths of the glass transition of the mixed PSAN20/PMMA phase in different blends. The broken curve is drawn as a guide to the eye for the data of the model blends with homogeneously mixed PSAN20/PMMA phase

that, regardless of the total composition, the PS blocks of SM97 are very homogeneously mixed with PPE in ternary blends of series 1, comparable with simple binary PS/PPE blends. From this we already have to expect that the ternary blends must have a very high degree of dispersion. The block copolymers are completely located at the interface, the blocks extending deeply into the corresponding phases. Most of the material of the PSAN20 and PPE phases is enriched by the respective blocks, and therefore T_g shifts occur that can be calculated from the weight ratio of blocks to corresponding component phase. In blends with approximately equal amounts of PSAN20 and PPE this is realized by a highly interpenetrated morphology with length scales below $\approx$ 50–70 nm (see for example in the first paper[16] the TEM micrographs of blends PSAN20/PPE (60:40) with 10 and 20 wt% of block copolymer SM78). In ternary blends with less PPE, the morphology is finely dispersed with typical length scales below $\approx$ 50–70 nm for the dispersed PPE phase, as will be demonstrated in blend series 3.

Besides the very high degree of dispersion, most probably thermodynamically induced stretching of the long block chains is the basis for the observed homogeneous mixing of blocks into the respective blend components. As discussed in the first paper[16], the enthalpic interaction between PS and PPE is more favourable than between PMMA and PSAN20. This could explain why, in these blends, owing to a stronger stretching of the PS block chains, the segmental homogeneity in the mixed PS/PPE phase is better than in the PSAN20/PMMA mixed phase. The observed broadening of the PSAN20 glass transition of blends C and D is an indication for this. The block lengths should also be important for the degree of mixing of block chains into the respective blend components. It is to be expected that, if the blocks get shorter, the mixing will be less uniform. This question is examined in the next blend series 2. Owing to the larger difference in T_g between PS and PPE, the analysis will mainly focus on the PPE glass transition.

Dynamic mechanical analysis of blend series 2

In blend series 2 the weight ratio of P(S-*b*-MMA) to PPE is kept at a constant value of 20:80, while the amount of the main component PSAN20 is varied. In going from composition G to H to composition I (see *Figure 1* and *Table 4*) the blend structure changes from a clearly dispersed morphology to a more bicontinuous one. *Figures 9a–c* show how the glass transitions (tan δ_{max}) in these blends (G–I) change, as the molecular weight of the block copolymers is raised. As a reference, the upper curves in *Figures 9a–c* always correspond to the binary blend without block copolymer. From SM8 to SM120 the block copolymer molecular weight is successively increased, while the total chemical composition of the blends remains constant. Comparing the different blends of series 2, the influence of the block copolymer molecular weight is the same in compositions G, H and I. The short block copolymers SM8 and SM25 do not cause detectable alterations in the PPE glass transition. However, in blends with the larger block copolymers SM78, SM97 and SM120, the glass transition of the PPE phase is

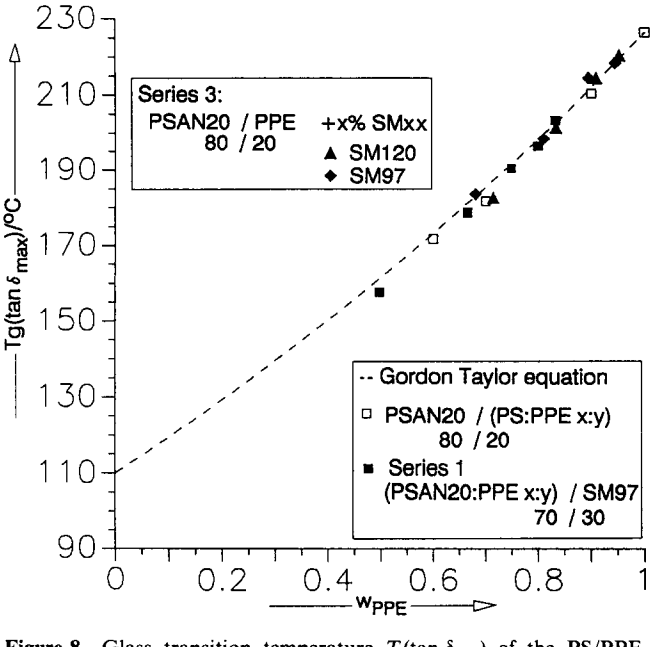

Figure 8 Glass transition temperature $T_g(\tan \delta_{max})$ of the PS/PPE mixed phase in different blends plotted against the fraction w_{PPE} based upon PS/PPE. The broken curve shows the prediction of the Gordon–Taylor equation (equation (1))

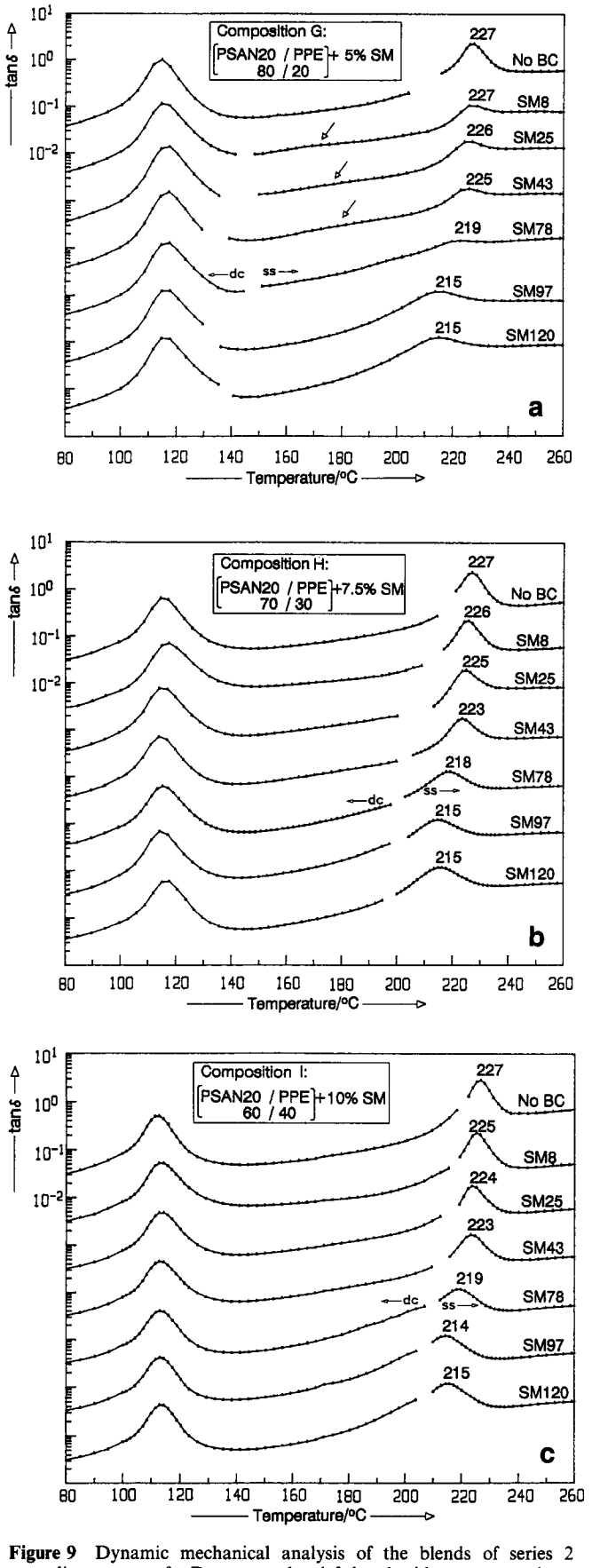

Figure 9 Dynamic mechanical analysis of the blends of series 2 according to tan δ. Data on the left-hand side correspond to measurements with the dual cantilever test fixture (dc), data on the right correspond to shear sandwich measurements (ss). The upper curve always corresponds to the binary blend without block copolymer. Curves of the different blends are vertically offset against each other by one decade. (a) Composition G: PSAN20/PPE (80/20) + 5% SM*xx* (x = 8–120). (b) Composition H: PSAN20/PPE (70/30) + 7.5% SM*xx*. (c) Composition I: PSAN20/PPE (80/20) + 10% SM*xx*

significantly lowered and somewhat broadened. The block copolymer SM43 shows behaviour between these extremes, i.e. the temperature reduction of the PPE glass transition is smaller and broadening occurs. All blends of series 2 do not show significant changes at the PSAN20 glass transition. The difference in T_g between PSAN20 and PMMA is only 35°C (PSAN20 tan δ_{max} = 111°C, PMMA tan δ_{max} = 136°C, see *Figure 4* and *Table 5*). In the blends of series 2 the fraction of PMMA in the potential PSAN20/PMMA mixed phase is low, ranging from 0.030 to 0.077. Therefore, as can be estimated from the Gordon–Taylor equation (broken curve in *Figure 6*), the enhancement of T_g in the PSAN20 phase by the PMMA blocks can at most be in the range of 1 to 2°C (in the case of complete homogeneous mixing).

The alterations of the PSAN20 glass transition by the presence of PMMA were discussed in series 1, in which the fraction of PMMA blocks was higher (higher amount of block copolymer). In series 2 the ternary blends with the *large* block copolymers show reductions in the glass transition temperature of the PPE phase comparable to binary blends of PS and PPE of corresponding compositions, the same behaviour as observed in blend series 1. The T_g of the mixed phase of PPE and PS blocks depends only on the ratio of PPE to block PS. The width of the glass transition is also comparable to that in the blends with homogeneously mixed homo-PS/PPE phase (*Figure 3*). This strongly supports the idea that, in ternary blends with large block copolymers, PS blocks and PPE are very homogeneously intermixed with very small dimensions of the phases.

As will be demonstrated in blend series 3, the dispersing efficiency of the different block copolymers is very high and not much different for different block copolymers. All blends of composition G with different block copolymers have typical dimensions of the highly dispersed PPE phase of less than $\approx$ 80 nm (see for example *Figure 13h*). Even the shortest block copolymer SM8, which is not microphase separated in the bulk state (homogeneous according to SAXS[22] and consistent with literature data[23]), showed approximately the same dispersing efficiency as the larger block copolymers. Though the short block copolymers have very good dispersing efficiency, no influence on the T_g of the PPE phase is detectable. Nevertheless, the strong dispersing effect and the results from series 3 strongly suggest that the short block copolymers are also completely located at the interface. Owing to the short block length, the penetration depth into the corresponding phases is low and PS block chains are only intermixed in the outer regions of the PPE particles. Most probably, rather strong segment density gradients exist in this outer zone and therefore the relaxation of this material is very broad and cannot be detected. The inner core of the PPE particles consists of pure PPE material whose glass transition is detected at 227°C as in blends without block copolymers. This combination of a narrow transition of pure PPE material and the broad relaxation of the intermixed zone gives the tan δ curves of the blends with short block copolymers in *Figures 9a–c*.

Figure 10 shows a schematic representation of possible types of segmental distributions across the PPE particles and their influence on the glass transition of the PPE phase. *Figure 10a* corresponds to the situation of blends with short block copolymers. Particles consist of an inner core region of pure PPE and an outer shell of intermixed

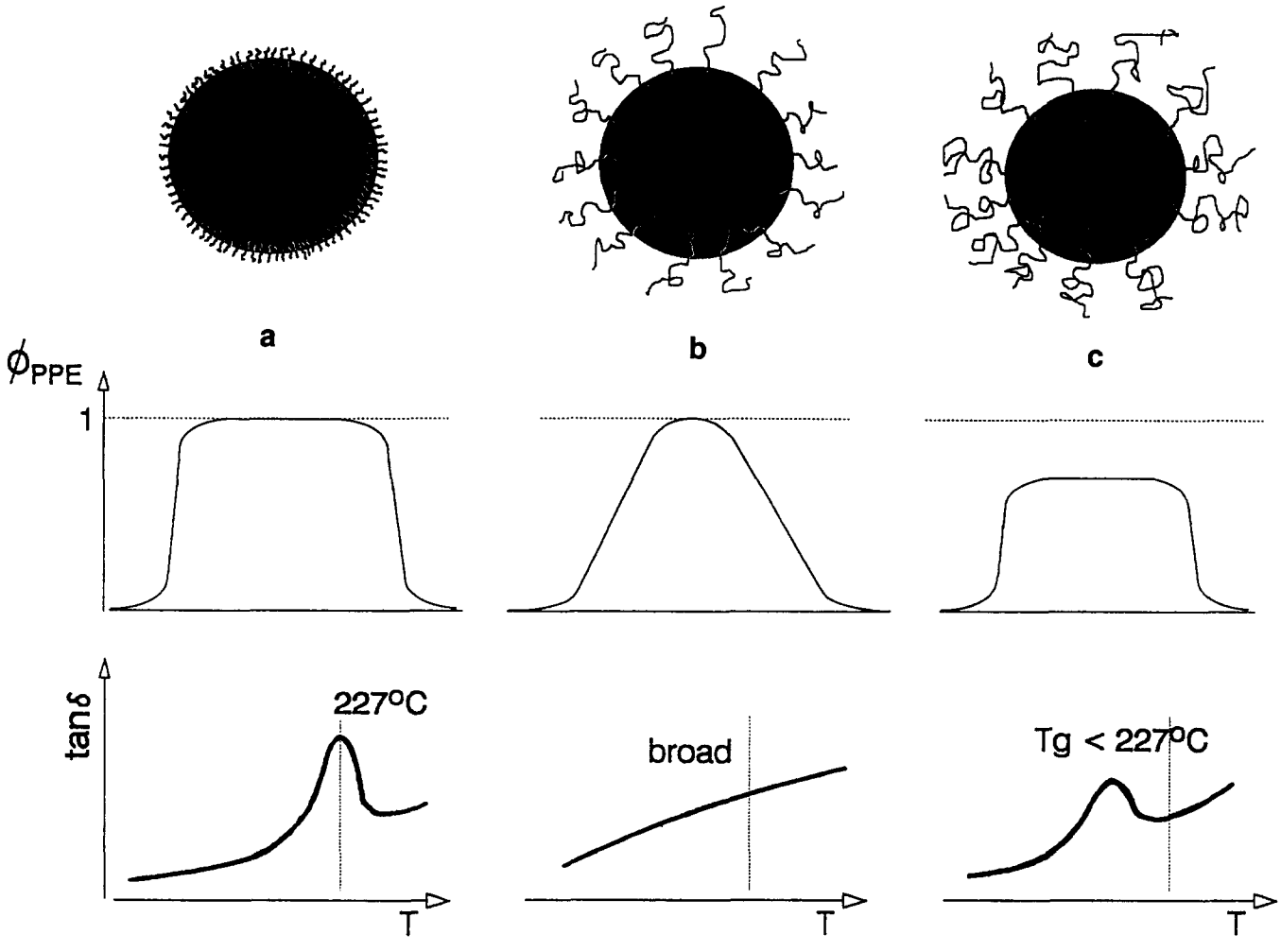

Figure 10 Schematic representation of different types of segmental distributions across the PPE phase (dark) in ternary blends PSAN20/PPE/P(S-*b*-MMA) and their influence on the PPE glass transition. ϕ_{PPE} = PPE segment density relative to pure PPE; differences in the particle dimensions are not considered. (a) Short block copolymers; particles consist mainly of pure PPE. (b) Strong segment density gradients across the whole PPE phase lead to very broad glass transitions. (c) Large block copolymers; rather uniform segmental mixing and lowering of T_g predictable from the ratio of *b*-PS/PPE

PS blocks and PPE. *Figure 10c* describes the situation of blends with large block copolymers in which the PS blocks penetrate the whole PPE phase and create a rather uniform segment density distribution and therefore a reduction in T_g predictable from the ratio PS/PPE. Owing to the rather uniform segmental distribution, only moderate broadening of the glass transition is observed. *Figure 10b* depicts the situation with large segment density gradients across the whole PPE phase and therefore an extremely broadened glass transition. This behaviour is observed in some blends of series 3 with high amounts of block copolymers.

Which of these segmental distributions will be realized depends in a complex manner on the total composition of the blends, the degree of dispersion and, most importantly, on the molecular weight of the block copolymers. In each case PS blocks and PPE are intermixed, corresponding to a 'wet brush situation'. In all compositions of series 2, large block copolymers lead to a rather uniform segmental distribution (*Figure 10c*) and the short block copolymers to the situation in *Figure 10a*. Comparison of the glass transition behaviour of the block copolymers SM8 to SM78 in *Figure 9a* shows that the glass transition at ≈227°C corresponding to pure PPE becomes weaker and a very broad relaxation between the PSAN20 glass transition and the PPE glass transition develops (see arrows in *Figure 9a*). Interpreted in terms of the schematic picture of *Figure 10a* this means that the amount of the inner core material of pure PPE decreases and the amount of the outer mixed zone with large segment density gradients increases as the PS blocks become longer. In the case of the blends with SM97 and SM120 the situation corresponds to *Figure 10c* with rather uniform mixing of PS blocks with PPE. The same conclusions can be drawn from blend compositions H and I (*Figures 9b* and *9c*); however, owing to the larger amount of PPE, the tan δ maximum does not decrease to the same extent. Again the block copolymers with intermediate molecular weights SM25, SM43 and SM78 show an increased damping between the PSAN20 and PPE transition zone.

The elastic modulus of a multiphase polymer system depends on the moduli of components, composition and the way in which the phases are arranged and mechanically coupled[24]. Therefore, the composite modulus in the region between the PSAN20 glass transition and the PPE glass transition (i.e. the temperature region in which the moduli of both components are very different) reflects effects of morphology and phase adhesion. As mentioned above, the morphologies of the ternary blends with the same overall chemical composition but different block

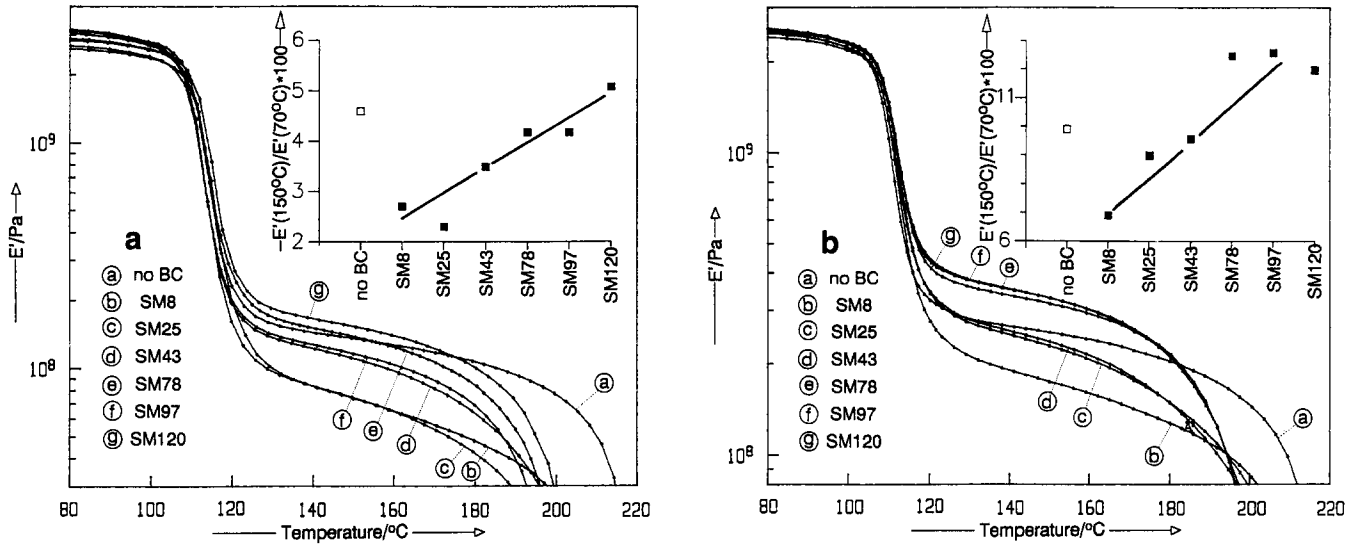

Figure 11 Temperature variation of the storage modulus E' as measured with the dual cantilever test fixture for the blends of series 2 ($xx = 8$–120). (a) Composition H: PSAN20/PPE (70:30) + 7.5% SMxx. (b) Composition I: PSAN20/PPE (60:40) + 10% SMxx. The inserts show the modulus at 150°C in per cent of the modulus at 70°C. The binary blends without block copolymers (a) are also included, although not directly comparable

copolymers are very similar. Therefore, the differences in modulus should be mainly due to the different extent of mechanical coupling.

Figures 11a and *11b* demonstrate the influence of block copolymer molecular weight in blends of composition H and I on the modulus E' as measured by the dual cantilever test fixture. Both compositions show the same trend: the 'plateau modulus' increases as the block copolymer molecular weight increases, i.e. phase adhesion is better in the blends with large block copolymers. In order to quantify this, the inserts in *Figures 11a* and *11b* show the value of E' at 150°C for the different blends in per cent of the value of E' at 70°C. Such a procedure eliminates possible errors on the absolute E' values due to errors in sample dimensions. The underlying assumption is that at 70°C all blends of identical composition (only differing in SM block copolymer) should have approximately the same modulus E' because morphologies are comparable and all components glassy (blends of composition *G* are not discussed because the 'plateau region' could not be covered with the dual cantilever test fixture). Also included in *Figures 11a* and *11b* are the respective curves for the binary PSAN20/PPE blends without block copolymer, although their behaviour is not directly comparable because morphology and overall composition are different. In contrast to the coarsely separated binary blends of PSAN20 and PPE, the ternary blends with block copolymers are very finely dispersed. Moreover the blends of composition I display an interconnected morphology (e.g. the TEM micrograph of the blend with SM78 of composition I is shown in our previous paper[16]).

Analysis of blend series 3 by d.m.a. and TEM

In blend series 3 the ratio of PSAN20 to PPE is kept constant at 80:20 (i.e. a morphology with clearly dispersed PPE phase) and the amount of different block copolymers varied from 2.5, 5 and 10 up to 20% (*Table 6*). These compositions were chosen to investigate in detail the effects of the molecular weight of the block copolymers on the glass transition of the PPE phase and morphology. Therefore, the following dynamic mechanical analysis will also be restricted to the temperature region above the

Table 6 T_g of mixed PS/PPE phase in blends of series 3[a]

	Compositions			
Copolymer BC (%) =	J 2.5	G 5	K 10	L 20
SM8	227	227	227(br)	br
SM25	226	226	223(br)	br
SM43	226	225	br	br
SM78	224	219	br	br
SM97	219	215	199	≈184
SM120	221	215	202	183

[a] T_g values correspond to the maximum (or centre) of the tan δ peak in *Figures 12a–f*; in some of the blends assessment was impossible because the peak was extremely broad (= br)

glass transition of the PSAN20 matrix, which is completely accessible with the shear sandwich test fixture. In all of these compositions the influence of the block copolymers on the PSAN20 glass transition is small and difficult to detect, because the ratio of PMMA to PSAN20 is very low (same reasons as discussed in blend series 2).

Figures 12a to *12f* show the variation in tan δ of the different compositions if the block copolymer is varied from SM8 to SM120. Depending on the overall composition and the molecular weight of the block copolymer, all situations outlined in *Figures 10a–c* are realized. For example, the blends with 2.5 and 5% of the shortest block copolymer SM8 (upper curves in *Figure 12a*) correspond to the situation in *Figure 10a*. The temperature of the PPE glass transition is practically unchanged. Most of the PPE particles consist of pure PPE. PS blocks and PPE are mixed with large segment density gradients only at the boundary regions. With increasing amounts of SM8, a broad relaxation attributable to a larger fraction of mixed PS/PPE phase is detected (see arrows in *Figure 12a*). At the same time the glass transition corresponding to pure PPE at 227°C gets weaker, i.e. the particles become smaller and therefore the relative amount of the outer region increases at the expense of pure PPE core material. In the blend with 20% SM8 (lower curve in *Figure 12a*) the glass transition of the mixed PS/PPE phase is extremely broadened and

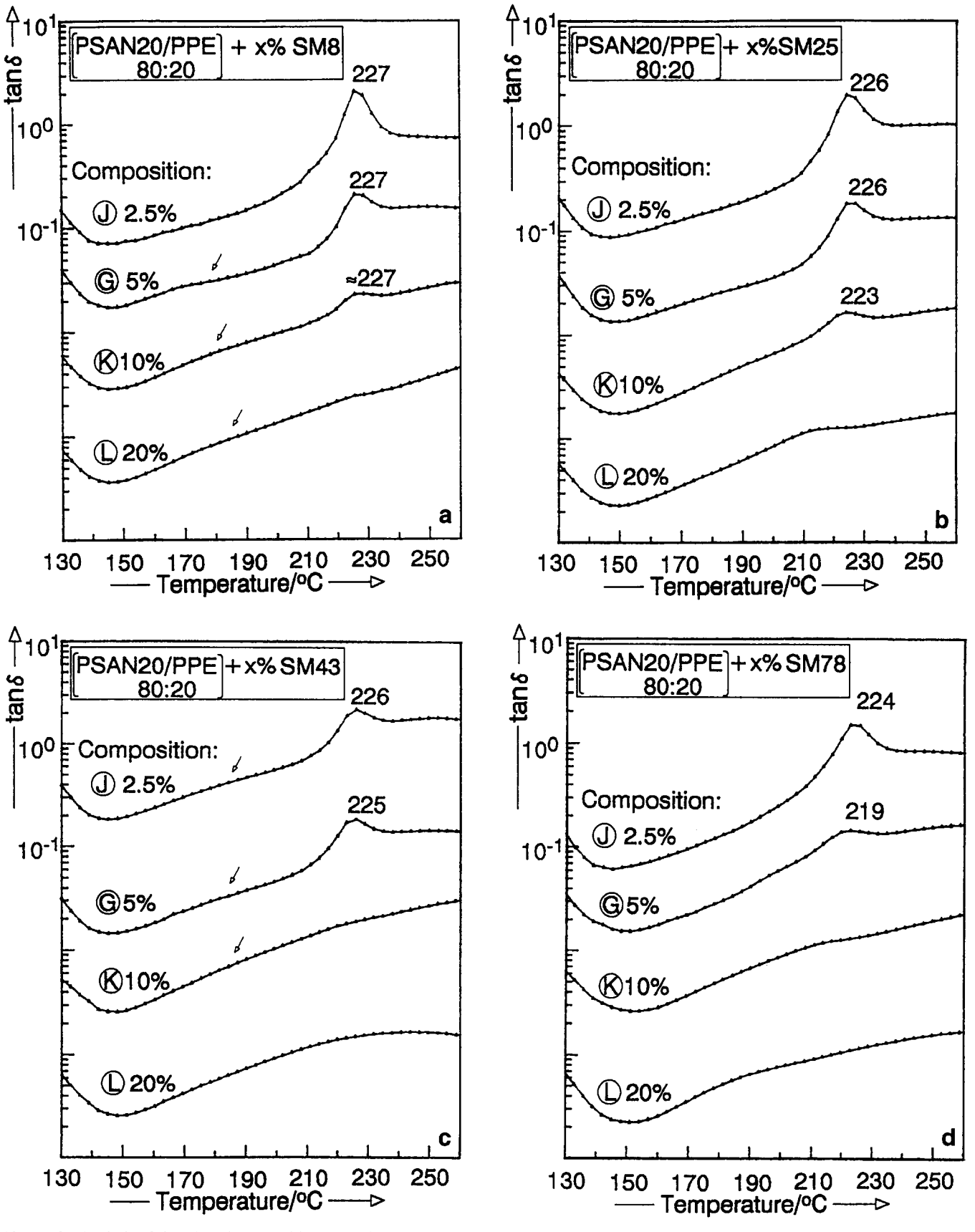

Figure 12 Analysis of the PPE glass transition according to tan δ of the blends of series 3 (measurements with the shear sandwich test fixture). Curves for different blends with the same block copolymer are vertically offset against each other by one decade. (a)–(f) Blends with different block copolymers

therefore hard to detect. Here the situation with large segment density gradients across the whole PPE phase, shown in *Figure 10b*, is realized.

Figures 13b and *13c* show TEM micrographs of the blends of *Figure 12a* with 2.5 and 20% of block copolymer SM8. Increasing the amount of SM8 from 2.5 to 20% strongly improves dispersion. The blends with block copolymer SM43 (*Figure 12c*) show a similar trend. At concentrations of 2.5 and 5 wt% the PPE glass transition remains nearly unchanged at 226°C, but relatively weak.

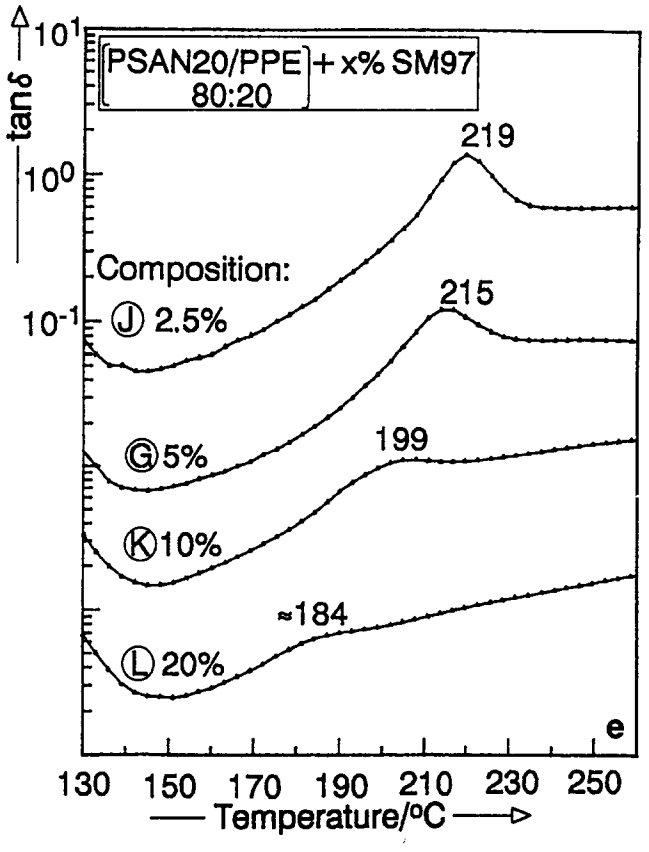

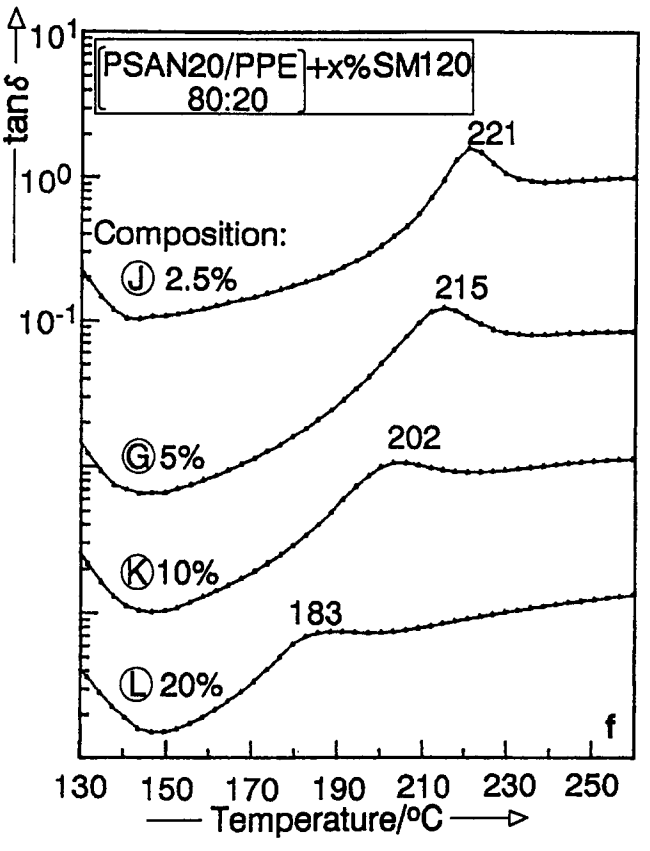

The outer shell of the PPE particles with mixed PS chains gives rise to the very broad transition at lower temperatures (arrows in *Figure 12c*). At the level of 10 and 20% block copolymer, the whole glass transition is extremely broad and nearly undetectable. These blends again correspond to the situation depicted in *Figure 10b* with large segment density gradients across the whole PPE phase. *Figures 13d–f* show the micrographs of blends with 2.5 and 20% SM43 to demonstrate the improvement in dispersion as the concentration of block copolymer is increased. *Figure 13f* gives a micrograph at higher magnification of the blend with 20% SM43.

In addition to the dynamic mechanical analysis, the micrographs further confirm that the low-molecular-weight block copolymers have high dispersing efficiency. No micelles or macrophase-separated block copolymers can be detected. If present, P(S-*b*-MMA) micelles dispersed in the PPE would be detectable as white spots in the PPE[16] under the staining conditions used throughout this study. Therefore, as already demonstrated for the larger block copolymers, all experimental evidence strongly supports that these small block copolymers are completely located at the interface with high interfacial activity in the sense of the dispersing efficiency. Similar effects of strong broadening of the PPE glass transition are also reported from binary blends of styrene–butadiene–styrene (SBS) triblock copolymers (with rather short PS end-blocks) with PPE[25]. The effect of broadening is also discussed in terms of concentration gradients of the PS and PPE segments across the mixed PS/PPE phase.

In all compositions of series 3 the larger block copolymers SM97 and SM120 show significant lowering of the PPE glass transition (*Figures 12e* and *12f*). At low concentrations the broadening of the glass transition is weak and comparable to the model blends with homogeneous mixed PS/PPE phase. At higher concentrations of the block copolymers SM97 and SM120 some broadening occurs, but not very pronounced (lower curves in *Figures 12e* and *12f*). It can be concluded that in all of these blends with large block copolymers the PS blocks are rather homogeneously mixed with PPE according to *Figure 10c*. At higher concentrations of these large block copolymers the segmental distribution also gets less uniform, but not as broad as in the case of the shorter block copolymers (lower curves in *Figures 12a–c*).

Representative for the blends with high-molecular-weight block copolymers, *Figures 13g–k* show the TEM micrographs of the blends of series 3 with the block copolymer SM97. Increasing the amount of block copolymer from 2.5 to 20% (*Figures 13g–j*) clearly improves dispersion, but between 5 and 20% the dispersing efficiency tends to level off. In the blend with 2.5% SM97 (*Figure 13g*) the PPE phase is very irregular in shape but clearly more dispersed than in the corresponding binary blend without block copolymer (*Figure 13a*). Besides higher dispersion, the PPE phase also becomes more spherical in shape in going from the blend with 2.5% SM97 to the blend with 20% SM97 (*Figures 13g–j*). *Figure 13k* gives a higher-magnification TEM micrograph of the blend with 20% SM97. As in all other blends, no micelles can be detected. In order to compare the dispersing efficiencies of the different block copolymers in the blends of series 3, a quantitative analysis was performed on some of these blends. In some blends the dispersed PPE phase is very irregular in shape (see for example *Figures 13a, b, d* and *g*) and therefore

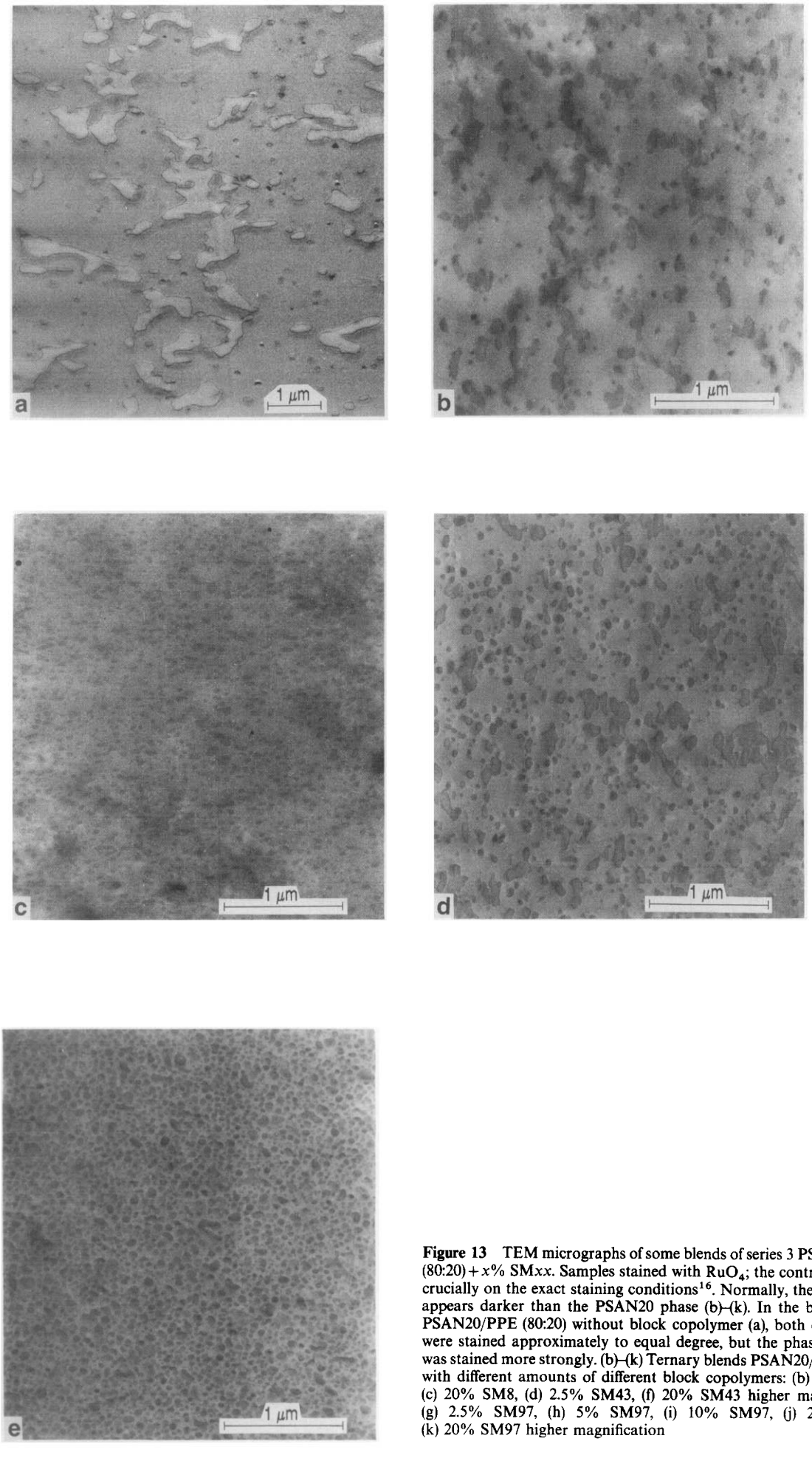

Figure 13 TEM micrographs of some blends of series 3 PSAN20/PPE (80:20) + x% SMxx. Samples stained with RuO_4; the contrast depends crucially on the exact staining conditions[16]. Normally, the PPE phase appears darker than the PSAN20 phase (b)–(k). In the binary blend PSAN20/PPE (80:20) without block copolymer (a), both components were stained approximately to equal degree, but the phase boundary was stained more strongly. (b)–(k) Ternary blends PSAN20/PPE (80:20) with different amounts of different block copolymers: (b) 2.5% SM8, (c) 20% SM8, (d) 2.5% SM43, (f) 20% SM43 higher magnification, (g) 2.5% SM97, (h) 5% SM97, (i) 10% SM97, (j) 20% SM97, (k) 20% SM97 higher magnification

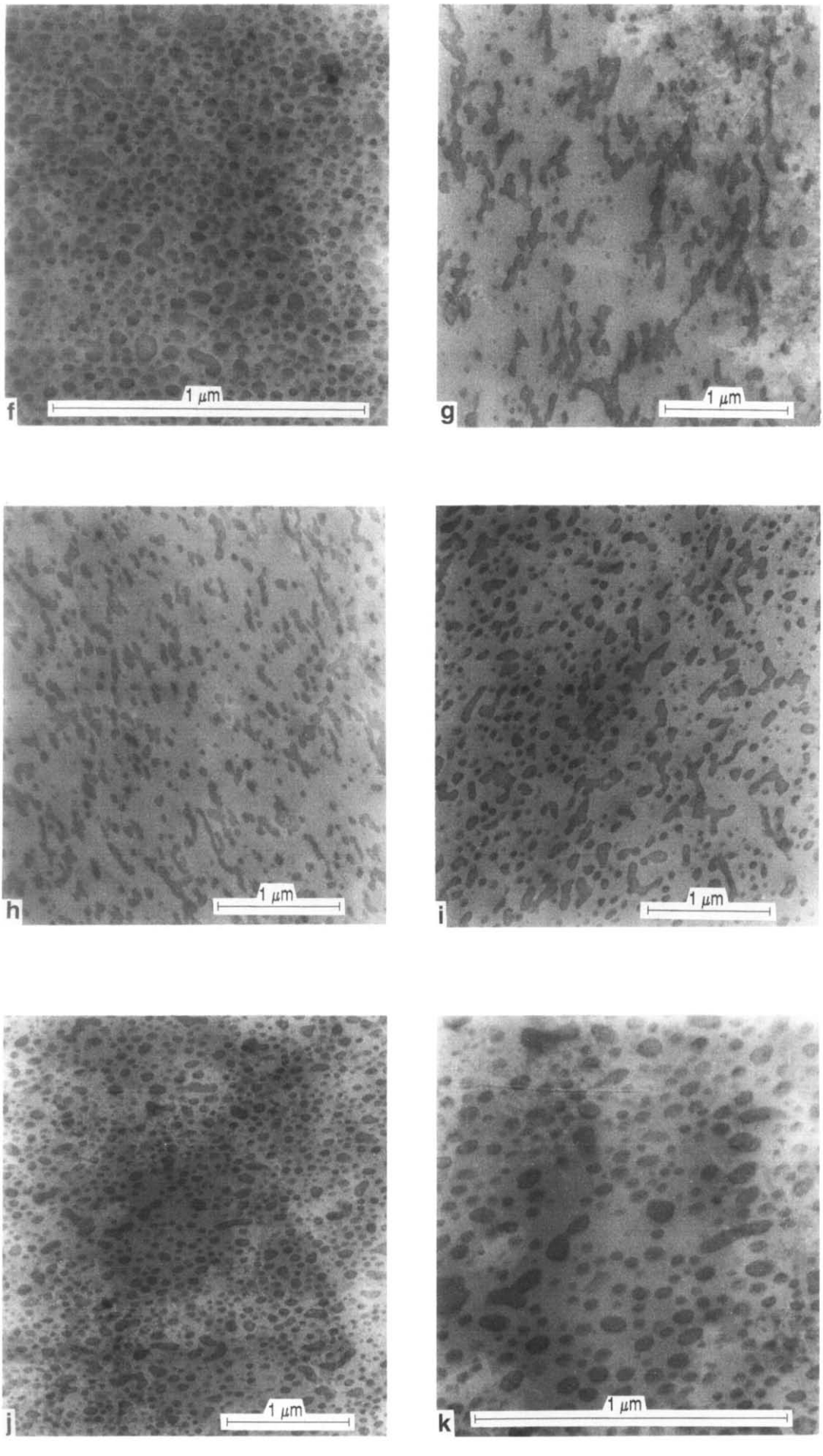

Figure 13 *continued*

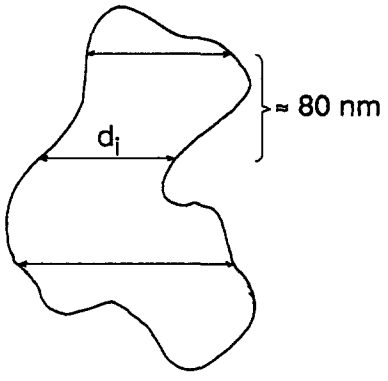

Figure 14 Procedure to characterize the typical dimensions of irregular particles by measuring arbitrary gridlines d_i

the assessment of apparent particle diameters would be tedious and inaccurate.

According to *Figure 14* the micrographs were overlaid with gridlines and the arbitrary lengths d_i through the particles measured. The distance between neighbouring gridlines was kept in the same range as the thickness of the thin sections (50–100 nm). The distribution of these lengths is used to characterize the morphology. Such a procedure favours the shorter dimensions more strongly, similar to the effect of the thin sectioning. Therefore, to compensate partially for this effect, a higher average of the distribution of d_i values, the 'weight-average' d_w of the lengths d_i, has to be considered:

$$d_w = \frac{\sum d_i^2 n_i}{\sum d_i n_i} \quad (2)$$

with d_i = measured penetration length and n_i = number of lengths d_i.

Another quantity accessible by this procedure is the particle density σ as determined from the micrographs. If particle dimensions are in the range of or smaller than the section thickness ($\approx$50 nm), σ is additionally enhanced due to the projection of particle and particle edges lying in the thin section. Nevertheless, despite some shortcomings, the quantities d_w and σ can be used to compare the typical dimensions and the degree of dispersion in the different blends.

Figure 15a gives the average dimension d_w of some of the blends of series 3. For the unmodified binary blend (TEM micrograph *Figure 13a*) d_w is about 410 nm. In the blends with 2.5% block copolymer d_w is reduced to 160 nm (SM97), 110 nm (SM8) and 90 nm (SM43). For all blends with more than 5% block copolymer the dispersion efficiency, given as the average dimension of particles, levels off. The degree of dispersion is roughly comparable for the blends with different block copolymers. Typical dimensions d_w of these blends are in the range between 50 and 100 nm, i.e. a very finely dispersed morphology. Detailed comparison of the values in *Figure 15a* indicates that the block copolymer SM43 with 'medium' molecular weight gives the highest degree of dispersion, higher than the large block copolymer SM97 and the small block copolymer SM8.

Comparing the apparent surface particle density σ in *Figure 15b*, this trend is more pronounced. It should be mentioned that this apparent particle density is no direct expression of the degree of dispersion. The value of σ also reflects the increasing amount of mixed PS/PPE phase with increasing block copolymer concentration. If the particle dimensions are in the range of or less than the thickness of the ultrathin sections, the value of σ is additionally enhanced due to projections of particles of different layers and sectioned particle edges. Thus, the strong variation of σ with block copolymer concentration reflects these effects together with a rather moderate decrease in average particle dimensions. Nevertheless, *Figure 15b* also demonstrates the superiority of the 'medium'-molecular-weight block copolymer SM43 in terms of the dispersing efficiency.

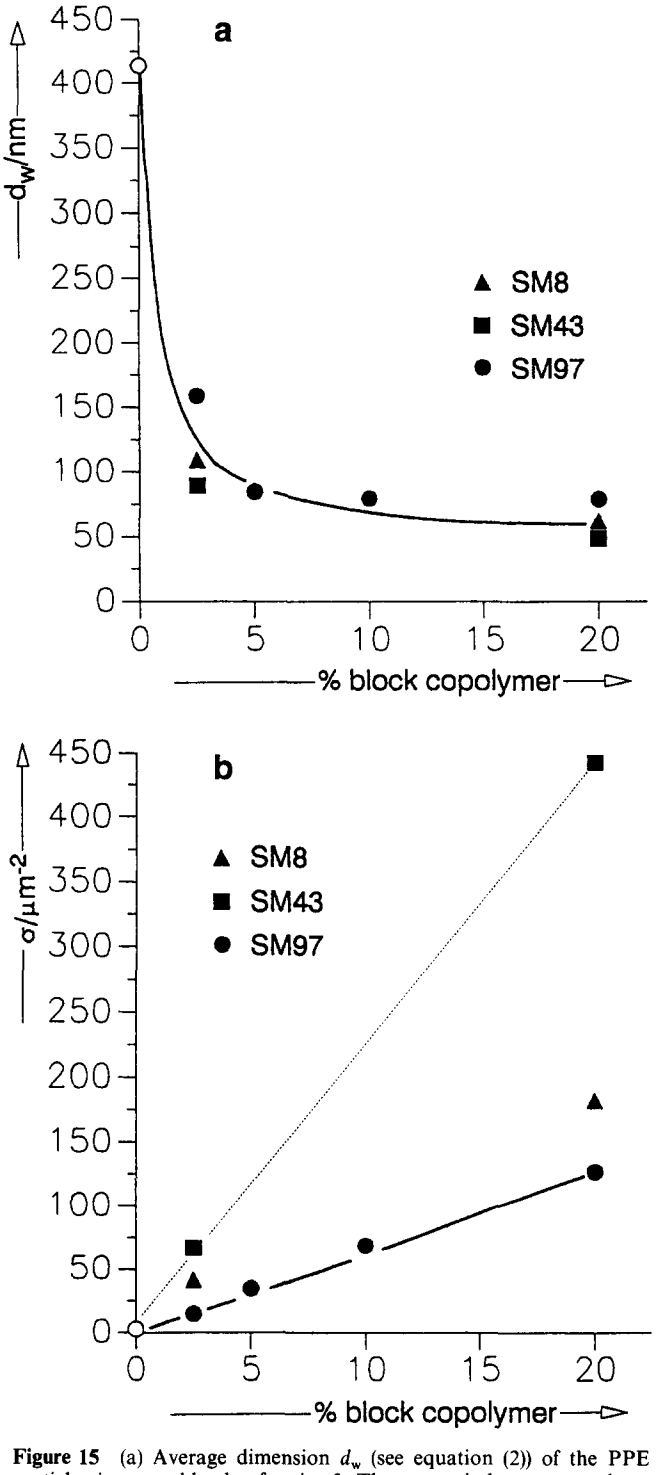

Figure 15 (a) Average dimension d_w (see equation (2)) of the PPE particles in some blends of series 3. The open circle corresponds to the binary blend PSAN20/PPE (80:20) without block copolymer. (b) Particle density σ (= number of particles/μm^2) for some blends of series 3 as determined from the micrographs; lines are drawn as a guide to the eye

The observed morphologies are in agreement with the qualitative model of segmental distribution (*Figure 10*).

All blends of series 3 with block copolymer concentrations from 5 to 20% show finely dispersed PPE particles with predominantly spherical shape (*Figures 13c, e, f* and *h–k*). The average dimensions are in the range between 50 and 100 nm. We can compare these dimensions with the typical dimensions of the block copolymers. First we assume that for these morphologies with spherical PPE particles the average dimension d_w is a good approximation of the average particle diameter. For a symmetric block copolymer P(S-*b*-MMA) with lamellar morphology, each block having a molecular weight of 100 000, the long period is about 66 nm and therefore the domain thickness is 33 nm[26]. The thickness of the interphase (≈ 5 nm) is rather broad. For comparison, the unperturbed radius of gyration of a PS homopolymer of molecular weight 100 000 is 8.7 nm[16].

According to d.m.a., PS blocks and PPE are rather homogeneously mixed in blends with the large block copolymers. This requires that the PS blocks reach the whole PPE domain and are stretched rather than coiled as in the bulk block copolymer state. In the case of the blends with 5, 10 and 20% of the block copolymer SM97, d_w is between 85 and 78 nm. Direct comparison with the microdomain size of 33 nm in the bulk block copolymer suggests that the PS blocks are stretched by a linear expansion factor of about 2.5. This estimation is crude but nevertheless gives an estimate of the magnitude of the stretching effect required to create a uniform distribution of PS segments across the PPE particle. In the blend with 20% SM97 the average dimension d_w of the PPE particles is 79 nm. In the blend with the block copolymer SM43 with block lengths approximately half as long as SM97, d_w is 49 nm (compare *Figures 13f* and *13k*). In this case the particle dimensions roughly scale as $d_w \sim M_{PS}^{0.59}$, a behaviour similar to the scaling of coil dimensions under good solvent conditions[27] and also comparable to the scaling of block copolymer microdomains (exponent = 0.5 (ref. 28) to 0.67 (ref. 26), depending on the degree of segregation). Indeed, PPE can be regarded as a thermodynamically 'good solvent' for the PS blocks.

In these blends with high amounts of block copolymers with respect to the dispersed PPE phase, the blend morphologies seem to be dominated by the morphological behaviour of the block copolymers. From another point of view, the situation in these blends could also be regarded as solubilization of PPE in PS microdomains. The homogeneity of this solubilization, i.e. the segmental distribution, depends on block copolymer molecular weight. In A/A-B blends, solubilization of A homopolymers into A microdomains is restricted to homopolymer molecular weights smaller than the corresponding block of the copolymer[29]. In blends of styrenic block copolymers with PPE this restriction does not exist owing to the favourable interaction between PS and PPE[25].

The shortest block copolymer SM8 represents a curious exception, because it is not microphase separated in bulk, but clearly plays its role as an interfacial agent. Probably the favourable enthalpic interactions between PS and PPE *as well as* PMMA and PSAN20 are responsible for the location to the interface and prevent macrophase separation. For comparison, binary blends of SM8 and PPE are macrophase separated with a homogeneous block copolymer phase. A binary blend PPE/SM8 (80:20) is turbid and mixing of PS blocks with PPE is not detectable according to d.m.a. (in contrast, all binary blends with higher-molecular-weight P(S-*b*-MMA) are microphase separated, transparent and the mixing of PS blocks and PPE is clearly detectable)[30]. Thus, it seems that interaction with both PSAN20 *and* PPE is necessary to prevent macrophase separation of the short block copolymer SM8 in ternary blends. This also represents a rare example in which a block copolymer that is not microphase separated undergoes phase separation of the blocks by the addition of *two* chemically different polymers which are selectively miscible with each of the blocks.

The morphology of the ternary blend with SM97 (*Figure 13g*) in comparison with the observed dynamic mechanical behaviour requires explanation. The PPE particles are rather large and very irregular. The average dimension d_w of these particles was determined to be 159 nm. D.m.a. demonstrated that PS blocks and PPE are homogeneously mixed (upper curve in *Figure 12e*). At first glance, this would suggest that the PS blocks are more strongly stretched than in the more highly dispersed blends with higher concentration of SM97, but another reasonable explanation is based on the strong irregularity of the particles. Owing to this irregularity, at each point in the particles there are short distances to the boundary in the range of ≈ 50–100 nm, i.e. most of the PPE phase is accessible by the PS chains without significantly stronger stretching as in the case of the blends with the smaller more spherical PPE particles. Thus, for these irregular morphologies the d_w value is not representative for the short scale dimensions of these rather large irregular particles. This situation is sketched in the schematic picture of *Figure 16*.

The exothermic heat of mixing between PS and PPE, expressed in a relatively large negative segmental interaction parameter ($\chi_{PS,PPE} = -0.1$ (ref. 31)), is the driving force for the stretching of the PS block chains. This strong stretching of PS block chains into a 'wet brush' situation with PPE is also reported in another investigation and recognized as an effect of 'enthalpy-driven swelling' of the PS chains[32]. The stretching of the

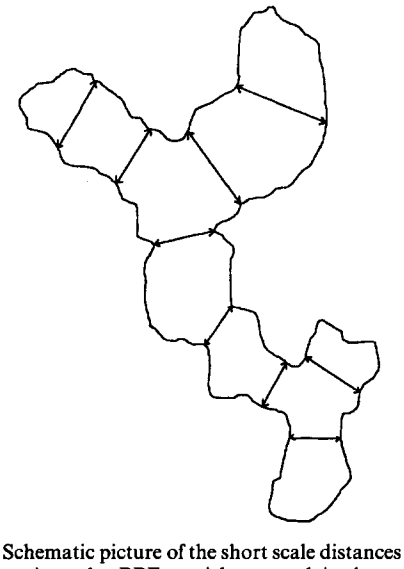

Figure 16 Schematic picture of the short scale distances in blends with relatively large irregular PPE particles to explain the extensive mixing of PS blocks and PPE

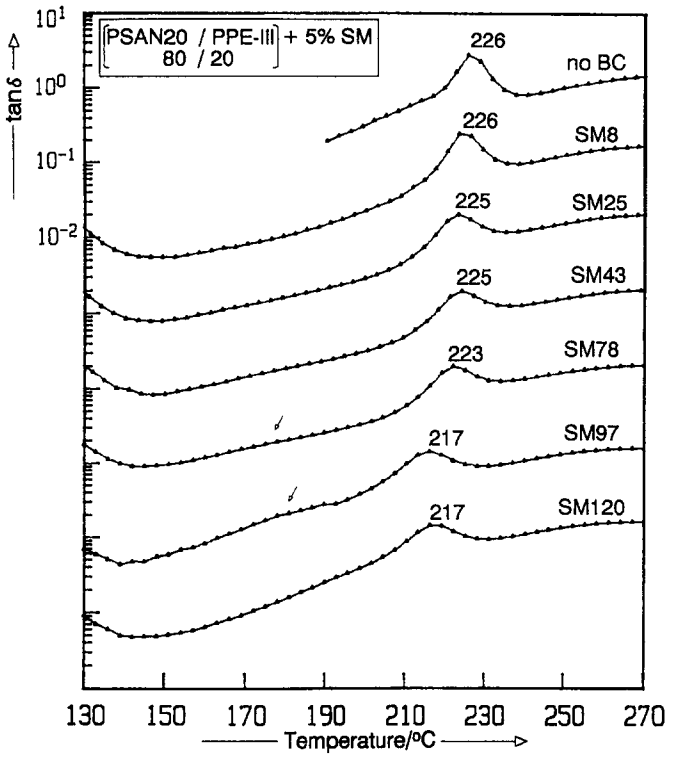

Figure 17 Analysis of the PPE glass transition in ternary blends of composition G with the low-molecular-weight PPE-III and different block copolymers (measurements with the shear sandwich test fixture). Curves of the different blends are vertically offset against each other by one decade

PS block chains of a high-molecular-weight P(S-*b*-MMA) block copolymer at the interface between PMMA and PPE was determined to be of the order of or greater than a factor of 2, a value very comparable to our rough estimation of ≈ 2.5. Theoretical predictions propose that much higher extensions may be possible[32]. It can be assumed that the PMMA chains that are mixed with PSAN20 will also be stretched to some extent, but most probably not as much as the PS brush on the PPE side, because the enthalpic interaction between PSAN20 and PMMA is less favourable ($\chi_{PSAN20,PMMA} \approx -0.008$)[16]. The dynamic mechanical analysis of blend series 1 supports these arguments. The glass transition behaviour of the PSAN20 phase indicates that, even in blends with the high-molecular-weight block copolymer SM97, the mixing of PSAN20 and PMMA blocks is not homogeneous.

Dynamic mechanical analysis of ternary blends with PPE of lower molecular weight

In this section we discuss the influence of the PPE molecular weight on the degree of segmental mixing of PS block chains and PPE. Ternary blends of PSAN20/PPE-III (80:20) with 5% of different block copolymers (composition G) were investigated in the temperature range above the PSAN20 glass transition with the shear sandwich test fixture. In comparison with the high-molecular-weight PPE-II ($M_n = 90\,000$) used in all preceding blends, the molecular weight of PPE-III ($M_n = 25\,000$) is significantly smaller by a factor of 3.6, but PPE-III has the same polydispersity (see *Table 2*).

Figure 17 shows the variation in tan δ of these blends with increasing block copolymer molecular weight. The upper curve corresponds to the binary blend without block copolymer (tan $\delta_{max} = 226$°C). Comparison of these blends with the corresponding blends with the high-molecular-weight PPE-II (*Figure 9a*) does not reveal significant differences. The low-molecular-weight block copolymers SM8–SM43 do not cause detectable lowering of the PPE glass transition. This corresponds to the segmental distribution outlined in *Figure 10a*. In the blends with the large block copolymers SM97 and SM120, $T_g(\tan \delta_{max})$ is lowered, as can be calculated from the ratio of PS to PPE, i.e. the extent of mixing is rather homogeneous.

The detailed comparison of *Figures 17* and *9a* reveals some minor differences. In the blends with SM78 and SM97 the broad relaxation attributed to the outer shell of the PPE particles with relatively large segment density gradients can be seen at lower temperatures (arrows in *Figure 17*). This indicates that, in contrast to blends with PPE-II, slight differences in the segmental distribution exist, but the overall behaviour is nearly the same. With increasing block copolymer molecular weight, a transition occurs from the segmental situation sketched in *Figure 10a* to the situation with rather homogeneous segmental mixing in *Figure 10c*. It can be concluded that the molecular weight of the PPE in the investigated range has no significant influence on the overall blend behaviour and also no drastic effect on the state of segmental mixing of PS block chains with PPE. The enthalpic interaction between PS and PPE seems to dominate the entropic contributions encountered with a change in the molecular weight of PPE. This insensitivity of the blend behaviour with respect to the PPE transition has also been reported for blends of styrenic triblock copolymers with PPE and attributed to the dominance of the enthalpic interactions[25]. Contrarily, in A/A-B blends of block copolymers with homopolymers that are chemically identical to the blocks, the ratio of block molecular weight to homopolymer molecular weight decisively determines the phase behaviour[33].

CONCLUSIONS

Owing to the carefully chosen preparation conditions, the blends can be expected to be close to equilibrium. Annealing experiments within the range of thermal stability of the PMMA block (annealing for several hours at $T = 240$°C) gave no indication of significant changes in the dynamic mechanical and morphological behaviour of the ternary blends. It was demonstrated that, independent of molecular weight, all symmetric block copolymers are located to the interface with strong dispersing efficiency. Even the lowest-molecular-weight block copolymer SM8, which is not microphase separated in bulk, shows high interfacial activity. PS blocks are mixed with PPE and PMMA blocks mixed with PSAN20, i.e. the block copolymers are arranged at the interface in a 'wet brush' situation. In blends with large block copolymers, the dynamic mechanical analysis reveals rather homogeneous mixing of PS blocks and PPE. The extent of mixing between PMMA blocks and PSAN20 seems to be less uniform. The PS chains are significantly stretched, approximately by a factor of 2.5. The favourable enthalpic interaction between PS and PPE is the driving force for this swelling. In ternary blends with short block copolymers in moderate amounts, the PS blocks do not penetrate deeply into the PPE phase.

Therefore the glass transition of pure PPE is still observed. With increasing molecular weight of the block copolymers, the segmental distribution across the PPE phase changes to a more uniform one. Besides depending on the degree of dispersion and the block copolymer molecular weight, the segmental distribution also depends on the overall blend composition. All of these factors determine the segmental mixing of PS blocks and PPE in a rather complex manner. Different situations of segmental distribution can be used to rationalize the glass transition behaviour and the morphological analysis. In ternary blends the molecular weight of PPE does not play an important role in determining the blend phase behaviour. The segmental distribution of PS blocks and PPE was hardly affected by the variation of the PPE molecular weight. These results are in contrast to the well known systems A/A-B/B in which the blocks of the compatibilizer are chemically identical to the component phases. Strong dependence of the dispersing efficiency has been demonstrated for such systems[5,12]. We believe that the observed insensitivity of the dispersing efficiency on molecular weight is a consequence of the favourable enthalpic interactions of both blocks with the respective component phases. This strong enthalpic driving force for the location of the block copolymers to the interface will always outweigh entropic effects encountered with a change of the block copolymer molecular weight. In the first paper we demonstrated that this is also responsible for the lack of micelle formation up to very high block copolymer concentrations, even with high-molecular-weight block copolymers. There was no indication for the formation of micelles in any of the blends investigated here. Nevertheless, the mechanical coupling between the phases depends on the block copolymer's molecular weight. This is understandable because the degree of mechanical coupling of the phases will depend on the degree of entanglement of the blocks with the respective phases and therefore the high-molecular-weight block copolymers showed superior behaviour in the temperature region between the glass transitions.

ACKNOWLEDGEMENTS

We are very grateful to Dr K. Mühlbach and Dr F. Seitz (BASF, Ludwigshafen) for fruitful discussions and supply of PSAN samples. Dr W. Heckmann (BASF) is thanked for suggestions concerning staining procedures. We are also very much indebted to Mr R. Würfel for careful operation of the EM. Financial support from BMFT and BASF through project 03 M 4041 is gratefully acknowledged.

REFERENCES

1 Paul, D. R. 'Polymer Blends', Academic Press, New York, 1978, Vol. 1
2 Bucknall, C. B. 'Toughened Plastics', Applied Science, London, 1977
3 Teyssie, Ph. *Makromol. Chem., Macromol. Symp.* 1988, **22**, 83
4 Tessie, Ph., Fayt, R. and Jerome, R. *Makromol. Chem., Macromol. Symp.* 1988, **16**, 41
5 Noolandi, J. and Hong, K. M. *Macromolecules* 1982, **15**, 482
6 Noolandi, J. and Hong, K. M. *Macromolecules* 1984, **17**, 1531
7 Leibler, L. *Makromol. Chem., Macromol. Symp.* 1988, **16**, 1
8 Shull, R. K. and Kramer, E. J. *Macromolecules* 1990, **23**, 4769
9 Banaszak, M. and Whitmore, M. D. *Macromolecules* 1992, **25**, 249
10 Lindsey, C. R., Paul, D. R. and Barlow, J. W. *J. Appl. Polym. Sci.* 1981, **26**, 1
11 Fayt, R., Jerome, R. and Teyssie, Ph. *J. Polym. Sci., Polym. Phys. Edn.* 1982, **20**, 2209
12 Anastasiadis, S. H., Gancarz, I. and Koberstein, J. T. *Macromolecules* 1989, **22**, 1449
13 Shull, K. R., Kramer, E. J., Hadziioannou, G. and Tang, W. *Macromolecules* 1990, **23**, 4780
14 Russel, T. P., Anastasiadis, S. H., Menelle, A., Felcher, G. P. and Satija, S. K. *Macromolecules* 1991, **24**, 1575
15 Dai, K. H., Kramer, E. J. and Shull, K. R. *Macromolecules* 1992, **25**, 220
16 Auschra, C., Stadler, R. and Voigt-Martin, I. G. *Polymer* 1993, **34**, 2081
17 Jones, R. A. L., Norton, L. J., Shull, K. R., Kramer, E. J., Felcher, G. P., Karim, A. and Fetters, L. J. *Macromolecules* 1992, **25**, 2359
18 Shull, K. R. and Winey, K. I. *Macromolecules* 1992, **25**, 2637
19 Halperin, A., Tirell, M. and Lodge, T. P. *Adv. Polym. Sci.* 1992, **100**, 32
20 Auschra, C. and Stadler, R. *Polym. Bull.* in press
21 de Araujo, M. A., Stadler, R. and Cantow, H. J. *Polymer* 1988, **29**, 2235
22 Gleinser, W. Diploma Thesis, Freiburg, 1990
23 Russel, T. P., Hjelm, R. P. and Seeger, P. A. *Macromolecules* 1990, **23**, 890
24 Dickie, R. A. in ref. 1, p. 353
25 Tucker, P. S., Barlow, J. W. and Paul, D. R. *Macromolecules* 1988, **21**, 1678, 2794
26 Green, F. P., Russel, T. P., Jerome, R. and Granville, M. *Macromolecules* 1988, **21**, 3266
27 De Gennes, P. G. 'Scaling Concepts in Polymer Physics', Cornell University Press, Ithaca, NY, 1979
28 Leibler, L. *Macromolecules* 1980, **13**, 1602
29 Inoue, T., Soen, T., Hashimoto, T. and Kawai, H. *Macromolecules* 1980, **3**, 87
30 Auschra, C. *Doctoral Dissertation* Mainz, 1992
31 Kambour, R. P., Bendler, J. T. and Bopp, R. C. *Macromolecules* 1983, **16**, 753
32 Brown, H. R., Char, K. and Deline, V. R. *Macromolecules* 1990, **23**, 3383
33 Roe, R. J. and Rigby, D. *Adv. Polym. Sci.* 1987, **82**, 103